

# NEW OBSERVATIONS AND A POSSIBLE DETECTION OF PARAMETER VARIATIONS IN THE TRANSITS OF GLIESE 436b

JEFFREY L. COUGHLIN<sup>1</sup>, GUY S. STRINGFELLOW<sup>2</sup>, ANDREW C. BECKER<sup>3</sup>, MERCEDES LÓPEZ-MORALES<sup>4</sup>, FABIO MEZZALIRA<sup>2</sup>, TOM KRAJCI<sup>5</sup>

*Draft version March 20, 2019*

## ABSTRACT

We present ground-based observations of the transiting Neptune-mass planet Gl 436b obtained with the 3.5-meter telescope at Apache Point Observatory and other supporting telescopes. Included in this is a detected transit in early 2005, over two years before the earliest reported transit detection. We have compiled all available transit data to date and perform a uniform modeling of all data using the JKTEBOP code. We do not detect any transit timing variations of amplitude greater than  $\sim 1$  minute over the  $\sim 3.3$  year baseline. We do however find possible evidence for a self-consistent trend of increasing orbital inclination, transit width, and transit depth, which supports the supposition that Gl 436b is being perturbed by another planet of  $\lesssim 12 M_{\oplus}$  in a non-resonant orbit.

*Subject headings:* planetary systems — stars: individual (Gliese 436)

## 1. INTRODUCTION

Gliese 436 is an M-dwarf (M2.5V) with a mass of  $0.45 M_{\odot}$  and hosts the extrasolar planet Gl 436b, which is currently the least massive transiting planet with a mass of  $23.17 M_{\oplus}$  (Torres 2007), and the only planet known to transit an M dwarf. Gl 436b was first discovered via radial-velocity (RV) variations by Butler et al. (2004), who also searched for a photometric transit, but failed to detect any signal greater than 0.4%. It was thus a surprise when Gillon et al. (2007b) reported the detection of a transit with a depth of 0.7%, implying a planetary radius of  $4.22 R_{\oplus}$  (Torres 2007) and thus a composition similar to Uranus and Neptune. In addition, two other peculiarities of the system warranted further investigation. Both Deming et al. (2007) and Maness et al. (2007) calculated that the significant eccentricity of the orbit,  $e = 0.15$ , coupled with its short period of  $\sim 2.6$  days, should result in circularization timescales of  $\sim 10^8$  years, which contrasts with the old age of the system at  $\gtrsim 6 \times 10^9$  years. Maness et al. (2007) also identified a linear velocity trend of  $1.36 \pm 0.4 \text{ m s}^{-1} \text{ yr}^{-1}$  in the RV data, indicating the presence of an outer body in the system with  $P \gtrsim 15$  years. The existence of one or more additional planets in the system could be responsible for perturbations to Gl 436b's orbit, and thus result in the observed peculiarities. We considered this possibility right after the initial publication of Gillon et al. (2007b), and began an intensive campaign to observe the photometric transits of Gl 436b in order to search for variations indicative of orbital perturbations (Stringfellow et al. 2008).

Early this year, Ribas et al. (2008a) reported the possible detection of a  $\sim 5 M_{\oplus}$  companion in the Gl 436 system located near the outer 2:1 resonance of Gl 436b via analysis of all the RV data compiled to date. Theoretically this planet would be perturbing Gl 436b so as to increase its orbital inclination at a rate of  $\sim 0.1 \text{ deg yr}^{-1}$ , and thus its transit depth and length, so that the non-detection by Butler et al. (2004) and the observed transit of Gillon et al. (2007b) were compatible. Since the RV detection of this second planet had a significant false-alarm probability of  $\sim 20\%$ , Ribas et al. (2008a) proposed that confirmation could be achieved through 2008 observations of Gl 436b's transits, which would show a lengthening of transit duration by  $\sim 2$  minutes compared to the Gillon et al. (2007b) data. As well, transit-timing variations (TTVs) on the order of several minutes should also be detectable by observing a significant number of transits.

Recently, Alonso et al. (2008) reported a lack of observed inclination changes and TTV evidence for the second planet, based on a comparison of a single H band light curve obtained in March 2008 to  $8\mu\text{m}$  data taken with Spitzer 254 days earlier (Gillon et al. 2007a; Deming et al. 2007). This result, combined with additional radial velocity measurements (Howard 2008; Bonfils 2008) that contradicted the proposed period of the second planet, drove Ribas et al. (2008b) to retract their claim of the companion at IAU Symposium 253. However, very recently Shporer et al. (2008) presented multiple light curves obtained in May 2007, and could not rule out TTVs on the order of a minute. While the planet specifically proposed by Ribas et al. (2008a) most likely does not exist, Ribas et al. (2008b) makes a strong case that a second planet is still needed to explain the peculiarities of Gl 436b, and most likely exists in a non-resonant configuration where no strong TTVs are induced. Amateur astronomers have been diligent in observing Gl 436b since its initial transit discovery, and thus along with this data, published data, and our own data, we are able to present a thorough analysis of the TTVs, inclination, duration, and depth of the transit

<sup>1</sup> Department of Astronomy, New Mexico State University, P.O. Box 30001, MSC 4500, Las Cruces, New Mexico 88003-8001; jlcough@nmsu.edu

<sup>2</sup> Center for Astrophysics and Space Astronomy, Department of Astrophysical and Planetary Sciences, 389 UCB, Boulder, CO 80309-0389

<sup>3</sup> Department of Astronomy, University of Washington

<sup>4</sup> Hubble Fellow, Department of Terrestrial Magnetism, Carnegie Institution of Washington

<sup>5</sup> Astrokolkhoz Observatory, PO Box 1351, Cloudcroft, NM 88317

changes in the Gliese 436 system. We present our observations in §2, our modeling and derivation of parameters in §3, and explore the observed TTVs and parameters of the system over time in §4.

## 2. OBSERVATIONS

We observed Gl 436 (11h42m11s, +26°42′24″ J2000) in the V filter on the nights of April 7, April 28, and May 6 2008 UT with the 3.5-meter telescope at Apache Point Observatory (APO). We used a backside-illuminated SITe 2048x2048 CCD with 2x2 binning and sub-framed to decrease readout time. We applied typical overscan, bias, and flat-field calibrations, the latter achieving very high signal-to-noise. For photometric reduction we used the standard IRAF task PHOT, with the photometric aperture selected as a constant multiple of the Gaussian-fitted FWHM of each image to account for any variable seeing. We performed differential photometry with respect to the star USNO 1167-0208653 (2MASS ID 175252970) located at 11h42m12.08s, +26°46′07.45″ J2000. This star has  $V=10.82$  and color  $V-I=1.48$ , compared to Gl 436 which has  $V=10.68$ , and color  $V-I=1.70$ . Having obtained at least 30 minutes of data on each side of the eclipse, we subtracted a linear fit for all data outside of eclipse vs. airmass to account for any differential reddening. Resulting individual data points have typical errors of about 1 mmag, with typical cadence of about 17 seconds with individual exposure times ranging from 0.8s-1.5s, depending on the nightly conditions. The three transits are shown in Figure 1. The  $\sim 10$  minute data gap seen for the May 6 transit during egress resulted from an instrument hang-up that required an instrument restart.

We also carried out accompanying observations with the New Mexico State University (NMSU) 1-meter telescope at APO, in the V filter on the night of April 7 2008 UT, and in the I filter on the night of April 28 2008 UT. A 2048x2048 E2V CCD was used with 2x2 binning and sub-framing, and we applied the aforementioned standard calibration and photometric extraction techniques. We performed ensemble photometry with respect to the USNO star that was used as the 3.5m reference, as well as BD+27 2046 ( $V=10.64$ ,  $V-I=0.44$ ), and another star at 11h42m00s, +26°45′56″ J2000 ( $V=12.81$ ,  $V-I=1.46$ ). Resulting typical errors on individual points were about 2 mmag with a typical cadence of about 12 seconds.

The NMSU 1-meter telescope can also function as a robotic telescope, and is used intermittently to photometrically monitor stars with known radial-velocity discovered planets to search for transits. A search of the 1-meter archives revealed that it observed Gl 436 on the night of January 11 2005 UT, and with the precise ephemeris for Gl 436b that is now available by incorporating our 3.5-meter data (see §4) we found a transit signature within a minute of the predicted time with reasonable width and depth, as shown in Figure 1.

We also conducted observations on the nights of April 28 and May 13 2008 UT using a 24″ telescope located at the Sommers-Bosch Observatory (SBO) on the University of Colorado at Boulder campus, using an I filter. These observations also used a windowed chip and an exposure time to maximize signal-to-noise without saturating, and have comparable temporal resolution to the 3.5m and 1m telescopes due to a shorter readout time. As well, we used an unfiltered 11″ tele-

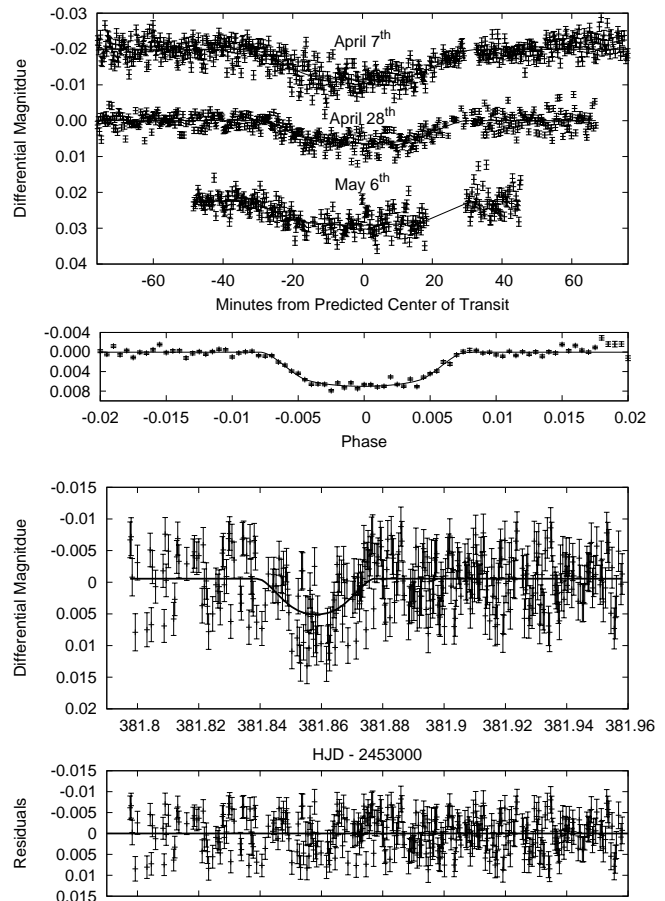


FIG. 1.— *Top*: The V band light curves observed with the APO 3.5-meter with model fits. Immediately below the data have been combined, phased, and binned in increments of 0.0005 phase. *Bottom*: The transit observed by the NMSU 1-meter telescope on the night of January 11 2005 UT. A 3-sigma clip has been applied, and is shown with a model fit for which the radii were fixed.

scope at Cloudcroft, NM (CC) with a SBIG ST-7E CCD and 2x2 binning on May 6 2008 UT, with a resulting cadence of about 25 seconds. Several other previous transits were observed and used to refine the observing technique that led to the transit detection of May 6, but due to higher noise are not included in this paper. We have also gathered all the amateur data currently available on the system as compiled by Bruce Gary (<http://brucegary.net/AXA/GJ436/gj436.htm>).

## 3. MODELING AND DERIVATION OF PARAMETERS

In order to perform a search for TTVs in the transit signature of Gl 436b, we compiled all the existing data from both professional and amateur astronomers available to date. We then used the JKTEBOP code (Southworth et al. 2004a,b) to model all the transit light curves in a consistent and uniform manner. Southworth (2008) has recently performed an exhaustive analysis of fourteen transiting planets using the JKTEBOP code, and showed it compared well with results reported elsewhere. JKTEBOP offers the advantage of incorporating a Levenberg-Marquardt optimization algorithm, improved limb darkening treatments, and extensive error analysis routines, which are critical for confirming any trends in the system.

For each transit curve, we solved for the ratio of radii ( $k = R_p/R_s$ ), the orbital inclination ( $i$ ), the time of mid-transit ( $T_0$ ), and a scale factor that defines the normalized value of the out-of-transit flux in the light curves. In order to obtain reasonable results for the scale of the system for all data sets, the sum of the radii ( $R_s + R_p$ ) was set to that found by Torres (2007). We also fixed the eccentricity to a value of 0.15 and the longitude of periastron to  $343^\circ$  as given by Deming et al. (2007) and Mardling (2008). We used a quadratic limb-darkening law with coefficients taken from Claret (2000) for  $T_{eff} = 3500\text{K}$ ,  $\log(g) = 4.5$ ,  $V_t = 2.0 \text{ km s}^{-1}$ , and  $[M/H] = 0.0$ , for the appropriate filters. In the case of the Spitzer  $8\mu\text{m}$  data, we used the coefficients as determined by Gillon et al. (2007a). From each fit, still assuming a constant sum of radii, we were thus also able to calculate the individual star and planet radii, as well as the depth and width of eclipse. In order to rule out any potential correlations in derived planet size and inclination, we then re-modeled all data with the same procedure, but also fixing  $k$ , and thus the star and planet sizes, to that found by Torres (2007). This generally produced similar results, but for the noisier data sets achieved more consistent results. Parameters from both techniques are shown in Table 1.

In order to obtain robust errors, we ran 1,000 Monte Carlo simulations for each data set and performed a residual-permutation analysis (Jenkins et al. 2002) to investigate temporally correlated noise. In both cases, the previously fixed parameters, as well as the limb-darkening coefficients, were allowed to vary so that their individual uncertainties would be taken into account in the derived parameter uncertainties. For each Monte Carlo simulation, random Gaussian noise with amplitude equal to the given error bars, or in the absence thereof the standard deviation of the residual scatter from the best-fit solution, was added to each data point and the curve re-fitted with random perturbations applied to the initial parameter values. This ensured a detailed exploration of the parameter space and parameter correlations. However, this Monte Carlo technique will underestimate errors for certain parameters in the presence of temporally correlated noise, which can result from trends in seeing, extinction, focus, or other atmospheric or telescope related phenomena (Southworth 2008). The residual-permutation method takes the residuals of the best-fit model, shifts them to the next data point, and finds a new solution. The residuals are shifted again, a new fit is found, and the process repeats as many times as there are datapoints. Thus we have a distribution of fitted values similar to the Monte Carlo technique, but any temporal trends will have been propagated around the light curve, and thus taken into account. For our final errors we adopt the larger value found between the two methods, although for the majority of parameters and data sets the two methods agree well.

In total we modeled 28 light curves, (15 professional and 13 amateur), covering 19 separate transit events over a baseline of nearly 3.3 years.

#### 4. TRANSIT TIMING AND ECLIPSE VARIATIONS

Using the derived time of minima in Table 1 for all the data when allowing  $k$  to vary, we derive a new linear, error-weighted ephemeris of  $T_c(\text{HJD}) = 2454222.6164(1)$

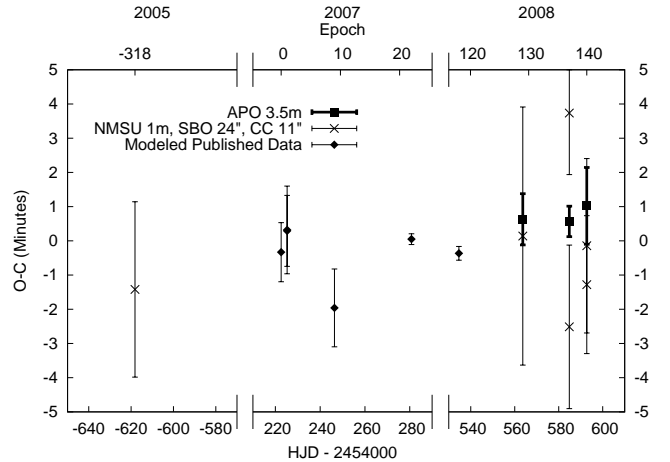


FIG. 2.— O-C diagram for all professional times of minima. Note the small error bars of the 3.5-meter observations.

+  $2.643898(2) \cdot E$ , where the parentheses indicate the amount of uncertainty in the last digit, and  $E$  is the epoch with  $E = 0$  the initial transit discovery of Gillon et al. (2007b). We note that the high-quality data from the 3.5-meter are primarily responsible for lowering the error in the period to less than ten times previously reported values (Alonso et al. 2008; Shporer et al. 2008). Using this ephemeris, we then compute an observed minus calculated (O-C) diagram for the time of transit center, as shown in Figure 2. We have currently excluded the amateur data from the plot due to much larger error bars, so that the high-precision data points can be seen clearly. We have examined the TTVs and various subsets thereof using a phase dispersion minimization technique (Stellingwerf 1978), but do not find any periods with statistical significance. Examining the best data, specifically the previously published data and our 3.5-meter observations, there is a standard deviation of 52 seconds. Assuming a sinusoidal TTV trend, we can then rule out any TTVs with amplitude greater than  $\sim 1$  minute.

We have searched for any trends in derived inclination, width, and depth of transit over time via error-weighted least-squares linear regression. In addition, we have also performed 10,000 Monte Carlo simulations for each fit, where gaussian noise with amplitude equal to each point's error bars was added in each iteration and the data re-fitted, with resulting  $1\sigma$  parameter distributions giving robust errors. The two methods agree to within 1% for all values. As mentioned in §3, we modeled all the light curves by both allowing the ratio of radii to vary as well as fixing it, and thus we list the values for each set. Performing fits to all the data, we have a tentative detection of increasing inclination and transit width with time, as shown in Table 2. We show these fits with the actual data derived when fixing the radii in Figure 3. As a precaution against any bias being introduced by the much larger number of data points at later epochs, we decided to separately bin the 2005, 2007, and 2008 data using an error-weighted mean, and re-fit the three resulting data points for each modeling method. As shown in Table 2, the values agree well with those derived when not binning the data.

The trends are moderately dependent on the single 2005 transit data point, which greatly extends the temporal baseline, and as such we are very cautious about

TABLE 2  
TRENDS IN DERIVED INCLINATION, WIDTH, AND DEPTH OF  
TRANSIT OVER TIME

Radii	Data Set	deg yr <sup>-1</sup>	min yr <sup>-1</sup>	mmag yr <sup>-1</sup>
Variable	All	0.119±0.062	3.39±1.01	-0.24±0.14
	Binned	0.127±0.062	3.52±0.97	-0.13±0.13
	No 2005	0.091±0.100	3.07±1.10	-0.28±0.15
Fixed	All	0.070±0.048	2.32±0.88	0.30±0.20
	Binned	0.072±0.049	2.35±0.85	0.31±0.20
	No 2005	0.018±0.099	1.70±1.29	-0.02±0.42

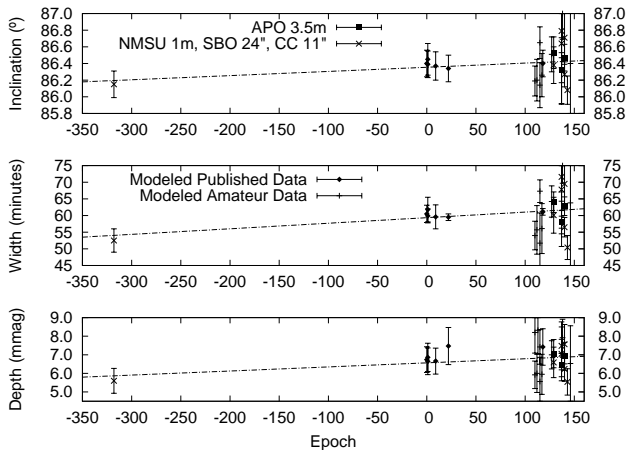


FIG. 3.— Measured inclination, width, and depth of transit over time for all data, with the star and planet radii fixed.

any claims. Resulting temporal trends when removing the 2005 data point are also shown in Table 2. Although while removing the 2005 data point significantly weakens the claim of a variation of inclination with time, the trend of increasing width still holds. Also of interest is that at a rate of 0.119 deg yr<sup>-1</sup>, as derived from our fit to all the data fitted with a variable radius, the JK-TEBOP program yields an increase in transit width of 4.364 min yr<sup>-1</sup>, and depth of 0.544 mmag yr<sup>-1</sup>, which for the inclination and width rates are in agreement with our observed trends, and thus are self-consistent. Since for the fixed radii rates the width and depth of eclipse are solely determined by inclination, we cannot make the same comparison. As well, the measured rate of inclination change is compatible the  $\sim 0.1$  deg yr<sup>-1</sup> required to make congruent the non-detection of Butler et al. (2004) and the observed transit of Gillon et al. (2007b). Extending the measurement baseline a couple years into the future will confirm or negate this result.

## 5. DISCUSSION AND CONCLUSION

We have presented a total of nine new transit light curves of Gl 436b, three of which come from the 3.5-meter telescope at Apache Point, and one of which is from the NMSU 1-meter in January 2005. We have collected and uniformly modeled all available professional and amateur light curves, and searched for any trends in transit timing, width of eclipse, or depth of eclipse variations. We find statistically significant, self-consistent trends that are compatible with the perturbation of Gl 436b by a planet with mass  $\lesssim 12 M_{\oplus}$  in a non-resonant orbit with semi-major axis  $\lesssim 0.08$  AU. This conclusion is based on the numerical simulations of Ribas et al. (2008a, see Fig. 1) who constrain the mass and semi-major axis of the theoretical second planet by examining which configurations could produce the observed orbital perturbations while still remaining undetected by the existing radial-velocity data. From our analysis, we infer a non-resonant orbit based on a lack of detected TTVs with amplitude  $\gtrsim 1$  minute. We stress that our measured trends are moderately dependent on our 2005 data, and thus subsequent high-precision observations over the next few years need to be carried out to confirm or refute this trend. Although the amateur observations are large in number, the very small depth of the transit makes it a challenge for most small aperture systems, resulting in very large uncertainties in  $i$  and  $T_0$ . If our trend is confirmed, it would be strong evidence for the first extrasolar planet discovered via orbital perturbations to a transiting planet.

**Acknowledgments.** JLC acknowledges support from the New Mexico Space Grant Consortium and the National Science Foundation, and GSS is supported by grants from NASA. MLM acknowledges support provided by NASA through Hubble Fellowship grant HF-01210.01-A awarded by the STScI, which is operated by the AURA, Inc., for NASA, under contract NAS5-26555. The authors would like to thank Eric Algol for helpful discussions, and Roi Alonso for providing his H band data. We also thank the many amateur astronomers for dedicated monitoring of the Gl 436 system, and to Bruce L. Gary for compiling their data. This research is based on observations obtained with the Apache Point Observatory 3.5-meter telescope, which is owned and operated by the Astrophysical Research Consortium, and has made use of the USNOFS Image and Catalogue Archive operated by the United States Naval Observatory, Flagstaff Station (<http://www.nofs.navy.mil/data/fchpix/>).

## REFERENCES

- Alonso, R., Barbieri, M., Rabus, M., Deeg, H.J., Belmonte, J.A., & Almenara, J.M. 2008, submitted to A&A, arXiv:0804.3030  
Bonfils, X. 2008, IAU Symposium 253  
Butler, R.P., Vogt, S.S., Marcy, G.W., Fischer, D.A., Wright, J.T., Henry, G.W., Laughlin, G., & Lissauer, J.J. 2004, ApJ, 617, 580  
Claret, A. 2000, A&A, 363, 1081  
Deming, D., Harrington, J., Laughlin, G., Seager, S., Navarro, S.B., Bowman, W.C., & Horning, K. 2007, ApJ, 667, L199  
Gillon, M., et al. 2007a, A&A, 471, L51  
Gillon, M., et al. 2007b, A&A, 472, L13  
Howard, A. 2008, IAU Symposium 253  
Jenkins, J.M., Caldwell, D.A., Borucki, W.J. 2002, ApJ, 564, 495  
Maness, H.L., Marcy, G.W., Ford, E.B., Hauschildt, P.H., Shreve, A.T., Basri, G.B., Butler, R.P., & Vogt, S.S. 2007, PASP, 119, 90  
Mardling, R. A. 2008, submitted to MNRAS, arXiv:0805.1928  
Ribas, I., Font-Ribera A., Beaulieu, J.-P. 2008a, ApJL, 677, L59  
Ribas, I., Font-Ribera, A., Beaulieu, J.-P., Morales, J.C., & García-Melendo, E. 2008b, to appear in the proceeds of IAU Symposium 253, arXiv:0807.0235  
Shporer, A., Mazeh, T., Winn, J.N., Holman, M.J., Latham, D.W., Pont, F., & Esquerdo, G. A. 2008, submitted to ApJ, arXiv:0805.3915

- Southworth, J., Maxted, P.F.L., & Smalley, B. 2004a, MNRAS, 351, 1277
- Southworth, J., Zucker, S., Maxted, P.F.L., & Smalley, B. 2004b, MNRAS, 355, 986
- Southworth, J. 2008, MNRAS, 386, 1644
- Stellingwerf, R. F. 1978, ApJ, 224, 953
- Stringfellow, G.S., Coughlin, J.L., López-Morales, M., Becker, A., Krajci, T., Mezzalana, F., & Algol, E. 2008, Cool Stars XV
- Torres, G. 2007, ApJ, 671, L65

TABLE 1  
PARAMETERS DERIVED FROM USING THE JKTEBOP CODE

Epoch	Source	Filter <sup>c</sup>	Tmin (HJD-2450000)	Inclination (deg)	R <sub>*</sub> (R <sub>☉</sub> )	R <sub>P</sub> (R <sub>☉</sub> )	Depth (mmag)	Width (minutes)
Ratio of Radii k Allowed to Vary								
-318	NMSU 1m	V	3381.85585±0.00178	86.02±0.23	0.446±0.046	6.23±4.88	7.10±1.31	46.9±7.2
0	Gillon et al. (2007b) <sup>b</sup>	V	4222.61617±0.00060	86.38±0.18	0.463±0.016	4.32±0.24	6.98±0.43	60.1±1.6
1	Shporer et al. (2008) <sup>b</sup>	None	4225.26052±0.00089	86.43±0.17	0.463±0.015	4.33±0.27	7.16±0.81	61.4±2.5
1	Shporer et al. (2008) <sup>b</sup>	V	4225.26050±0.00072	86.35±0.17	0.462±0.016	4.47±0.25	7.31±0.46	59.2±1.9
9	Shporer et al. (2008) <sup>b</sup>	R	4246.41012±0.00079	86.27±0.18	0.456±0.014	5.10±0.66	9.07±0.87	56.7±2.6
22	Gillon et al. (2007a)	8μm	4280.78219±0.00011	86.34±0.16	0.464±0.016	4.23±0.16	7.46±0.10	59.8±1.1
110	Gregor Srdoc <sup>a</sup>	R	4513.43393±0.00174	86.10±0.24	0.457±0.030	5.04±2.91	7.11±1.29	49.8±6.5
110	Tonny Vanmunster <sup>a</sup>	R	4513.44404±0.00247	87.13±0.30	0.461±0.016	4.57±0.45	9.63±1.67	77.8±4.9
112	Bruce Gary <sup>a</sup>	R	4518.72999±0.00278	86.04±0.34	0.443±0.087	6.55±9.38	8.78±2.37	47.0±11.7
113	Gregor Srdoc <sup>a</sup>	R	4521.37338±0.00130	87.27±0.30	0.459±0.015	4.81±0.30	11.06±1.13	80.0±4.2
115	James Roe <sup>a</sup>	V	4526.65995±0.00124	86.03±0.27	0.447±0.036	6.05±3.34	7.47±1.55	48.4±9.0
115	Joao Gregorio <sup>a</sup>	V	4526.65972±0.00130	87.09±0.28	0.468±0.016	3.80±0.25	6.50±0.66	77.1±4.0
117	Richard Schwartz <sup>a</sup>	V	4531.94399±0.00222	86.18±0.20	0.461±0.015	4.51±0.65	6.37±1.67	53.4±6.5
118	Alonso et al. (2008)	H	4534.59611±0.00014	86.39±0.17	0.463±0.016	4.32±0.17	7.74±0.11	61.1±0.9
127	Manuel Mendez <sup>a</sup>	R	4558.38849±0.00173	86.60±0.24	0.466±0.016	3.99±0.33	6.60±0.87	66.6±5.6
129	NMSU 1m	V	4563.67934±0.00262	86.45±0.34	0.467±0.018	3.87±0.64	5.74±1.10	62.1±8.2
129	APO 3.5m	V	4563.67968±0.00052	86.44±0.18	0.459±0.015	4.73±0.28	8.58±0.46	61.9±2.2
132	James Roe <sup>a</sup>	B	4571.61844±0.00107	88.60±0.62	0.455±0.015	5.24±0.24	14.84±0.83	95.5±3.6
137	NMSU 1m	I	4584.83302±0.00125	86.53±0.20	0.449±0.015	5.87±0.52	14.28±1.90	64.7±4.0
137	APO 3.5m	V	4584.83082±0.00031	86.32±0.16	0.464±0.016	4.20±0.20	6.36±0.13	58.2±1.2
137	SBO 24"	I	4584.82868±0.00166	86.63±0.21	0.448±0.015	5.95±0.50	15.23±2.13	67.3±3.8
137	Bruce Gary <sup>a</sup>	R	4584.82876±0.00087	86.51±0.18	0.463±0.015	4.32±0.25	7.41±0.58	64.0±2.4
138	Manuel Mendez <sup>a</sup>	R	4587.47754±0.00170	86.91±0.28	0.462±0.016	4.45±0.35	8.83±1.13	73.9±4.9
140	CC 11"	None	4592.76123±0.00140	86.25±0.17	0.463±0.015	4.38±0.48	6.64±1.03	56.0±3.4
140	APO 3.5m	V	4592.76283±0.00078	86.51±0.18	0.465±0.016	4.12±0.20	6.66±0.26	63.5±2.8
140	SBO 24"	I	4592.76202±0.00177	86.55±0.26	0.453±0.017	5.43±0.84	12.25±1.50	65.3±4.8
143	SBO 24"	I	4600.69795±0.00118	85.88±0.24	0.425±0.067	8.52±6.54	6.75±1.08	42.0±8.5
146	James Roe <sup>a</sup>	V	4608.62470±0.00107	86.32±0.23	0.454±0.015	5.31±0.67	9.86±0.55	58.4±6.3
...	3.5m Data Combined	V	...	86.39±0.17	0.463±0.015	4.36±0.23	7.09±0.34	60.2±1.8
Star and Planet Radii Fixed by Fixing k								
-318	NMSU 1m	V	3381.85602±0.00207	86.15±0.16	0.464±0.016	4.23±0.28	5.60±0.67	52.5±3.5
0	Gillon et al. (2007b) <sup>b</sup>	V	4222.61617±0.00062	86.40±0.16	0.464±0.016	4.23±0.28	6.74±0.69	60.5±2.6
1	Shporer et al. (2008) <sup>b</sup>	None	4225.26049±0.00094	86.45±0.19	0.464±0.016	4.23±0.30	6.86±0.76	61.8±3.7
1	Shporer et al. (2008) <sup>b</sup>	V	4225.26050±0.00076	86.39±0.16	0.464±0.016	4.23±0.30	6.65±0.72	59.9±2.1
9	Shporer et al. (2008) <sup>b</sup>	R	4246.41009±0.00103	86.37±0.17	0.464±0.017	4.23±0.29	6.66±0.70	59.6±3.6
22	Gillon et al. (2007a)	8μm	4280.78219±0.00011	86.34±0.16	0.464±0.016	4.23±0.30	7.47±1.00	59.5±1.0
110	Gregor Srdoc <sup>a</sup>	R	4513.43416±0.00191	86.19±0.18	0.464±0.016	4.23±0.28	5.92±0.74	54.0±4.3
110	Tonny Vanmunster <sup>a</sup>	R	4513.44424±0.00386	87.29±0.54	0.464±0.016	4.23±0.28	8.20±1.11	77.5±9.0
112	Bruce Gary <sup>a</sup>	R	4518.73038±0.00358	86.20±0.25	0.464±0.017	4.23±0.31	6.00±1.03	55.7±7.3
113	Gregor Srdoc <sup>a</sup>	R	4521.37312±0.00244	87.34±0.39	0.464±0.016	4.23±0.31	8.32±1.26	80.1±6.3
115	James Roe <sup>a</sup>	V	4526.66055±0.00302	86.14±0.27	0.464±0.015	4.23±0.28	5.56±1.30	51.7±9.1
115	Joao Gregorio <sup>a</sup>	V	4526.65996±0.00101	86.65±0.19	0.464±0.016	4.23±0.29	7.42±0.93	67.3±3.4
117	Richard Schwartz <sup>a</sup>	V	4531.94392±0.00198	86.26±0.26	0.464±0.016	4.23±0.31	5.95±1.08	56.1±7.5
118	Alonso et al. (2008)	H	4534.59610±0.00014	86.40±0.16	0.464±0.016	4.23±0.28	7.42±0.98	61.1±1.0
127	Manuel Mendez <sup>a</sup>	R	4558.38809±0.00164	86.51±0.21	0.464±0.016	4.23±0.23	7.00±0.76	64.2±4.7
129	NMSU 1m	V	4563.67961±0.00246	86.38±0.22	0.464±0.016	4.23±0.29	6.59±0.82	60.1±5.4
129	APO 3.5m	V	4563.67975±0.00117	86.53±0.19	0.464±0.016	4.23±0.28	7.06±0.76	64.0±3.1
132	James Roe <sup>a</sup>	B	4571.61831±0.00467	88.62±1.02	0.464±0.016	4.23±0.28	9.25±1.27	93.3±6.5
137	NMSU 1m	I	4584.83312±0.00424	86.79±0.87	0.464±0.016	4.23±0.29	7.48±1.29	71.6±17.1
137	APO 3.5m	V	4584.83082±0.00032	86.32±0.15	0.464±0.016	4.23±0.28	6.45±0.63	58.0±1.8
137	SBO 24"	I	4584.82787±0.00912	86.64±0.73	0.464±0.016	4.23±0.28	7.05±1.45	67.8±17.1
137	Bruce Gary <sup>a</sup>	R	4584.82874±0.00100	86.53±0.18	0.464±0.016	4.23±0.28	7.07±0.76	64.3±2.8
138	Manuel Mendez <sup>a</sup>	R	4587.47761±0.00204	87.00±0.31	0.464±0.016	4.23±0.29	7.92±0.99	75.0±5.3
140	CC 11"	None	4592.76119±0.00142	86.27±0.15	0.464±0.016	4.23±0.29	6.24±0.66	56.5±2.9
140	APO 3.5m	V	4592.76251±0.00089	86.47±0.16	0.464±0.016	4.23±0.29	6.92±0.75	62.8±2.8
140	SBO 24"	I	4592.76090±0.00430	86.71±0.32	0.464±0.016	4.23±0.28	7.57±1.06	69.5±7.8
143	SBO 24"	I	4600.69668±0.00171	86.08±0.17	0.464±0.016	4.23±0.30	5.54±0.71	50.4±3.6
146	James Roe <sup>a</sup>	V	4608.62542±0.00508	86.40±0.68	0.464±0.016	4.23±0.28	6.53±2.03	63.8±19.6
...	3.5m Data Combined	V	...	86.42±0.16	0.464±0.016	4.23±0.27	6.85±0.65	61.5±2.5

NOTE. — All errors are 1σ

<sup>a</sup> Amateur Observer with data obtained from Bruce Gary. <http://brucegary.net/AXA/GJ436/gj436.htm>

<sup>b</sup> Data were digitized from published plot

<sup>c</sup> Johnson-Cousins System